ORIGINAL ARTICLE

Planetary systems with forces other than gravitational forces

Søren Toxvaerd[1] (iD)

Abstract

A discrete and exact algorithm for obtaining planetary systems is derived in a recent article (Eur. Phys. J. Plus 2022, 137:99). Here, the algorithm is used to obtain planetary systems with forces different from the Newtonian inverse-square gravitational forces. A Newtonian planetary system exhibits regular elliptical orbits, and here, it is demonstrated that a planetary system with pure inverse forces also is stable and with regular orbits, whereas a planetary system with inverse cubic forces is unstable and without regular orbits. The regular orbits in a planetary system with inverse forces deviate, however, from the usual elliptical orbits by having revolving orbits with tendency to orbits with three or eight loops. Newton's Proposition 45 in *Principia* for the Moon's revolving orbits caused by an additional attraction to the gravitational attraction is confirmed, but whereas the additional inverse forces stabilize the planetary system, the additional inverse cubic forces can destabilize the planetary system at a sufficient strength.

Keywords Planetary systems · Inverse force dynamics · Inverse cubic force dynamics · Moon's revolving orbits

1 Introduction

Our world consists of objects with collections of atoms and molecules, which are bound together by ionic or covalent bonds. On a larger length scale, these objects are collected in the planetary systems in galaxies, which are bound together by gravitational forces. The ionic and covalent bonds are established by electromagnetic forces, whereas the planetary systems and the galaxies are hold together by gravitational forces. Although the two forces differ enormously in strength by a factor of $\approx 10^{36}$, they have, however, some common features. The radial strengths of both forces are proportional to the inverse square (ISF), r^{-2}, of the distances between mass centres, and both forces are believed to extend to infinity. The two

✉ Søren Toxvaerd
st@ruc.dk

1 Department of Science and Environment, Roskilde University, Postbox 260, 4000 Roskilde, Denmark

forces can also result in regular closed orbits for the dynamics of a collection of force centres, as is demonstrated by our solar system and the orbitals of the bounded electrons at an atomic nucleus. The two other fundamental forces are the strong and weak nuclear forces, and they are both short ranged. All other forces are "derived forces" such as the harmonic forces or the attractive induced dipole–dipole forces.

Isaac Newton formulated the classical mechanics in his book PHILOSOPHIÆ NATURALIS PRINCIPIA MATHEMATICA (*Principia*) (Newton 1726), where he also proposed the law of gravity and solved Kepler's equation for a planet's motion. According to Newton, gravity varies with the inverse square of the distance r between two celestial objects, and a planet exposed to the gravitational force from the Sun moves in an elliptical orbit. The Moon exhibits, however, periodic "revolving orbits" and Newton shows in *Principia* that this behaviour, which is caused by the daily rotation of the Earth, could be taken into account by and additional inverse cubic force proportional to r^{-3} (ICF). But it raises the question: for which forces can a system of objects have regular orbits?

It is only possible to solve the classical mechanics differential equations for two objects. The classical second-order differential equation for the dynamics of two objects with a central force proportional to r^n can be solved for a series of values of the power n. An important result was obtained by Bertrand (1873), who proved that all bound orbits are closed orbits. Later investigations have proved the existence of regular orbits for a series of values of the power n of the central force, including the ICF (Broucke 1980; Mahomed and Vawda 2000).

For a system consisting of many objects, the dynamics of coupled harmonic oscillators demonstrates that it indeed is possible to have stable regular dynamics for systems with other forces than the gravitational forces, but else there are no theoretical proofs, nor any other examples of that it is possible. Here, it is, however, demonstrated by molecular dynamics simulations (MD) of planetary systems (Toxvaerd 2022) that a planetary system also can have planets with stable regular orbits for attractive forces, which varies as

$$-r^{-1}$$
$$-r^{-2} \pm \alpha \times r^{-1}$$
$$-r^{-2} \pm \alpha \times r^{-3} \text{ for } \alpha \in [-100, 10].$$

But, it has not been possible to obtain stable regular orbits for r^{-3}.

2 The force between two spherically symmetrical objects

Newton was aware of that the extension of an object can affect the gravitational force between two objects, and in *Theorem XXXI* in *Principia* [8], he also solved this problem for ISF between spherically symmetrical objects.

Newton's *Theorem XXXI* states that:

1. A spherically symmetrical body affects external objects gravitational as though all of its mass were concentrated at a point at its centre.
2. If the body is a spherically symmetric shell, no net gravitational force is exerted by the shell on any object inside, regardless of the object's location within the shell.

Newton's theorem is, however, only valid for ISF. The forces between spherically symmetrical objects with forces proportional to r^{-1}, inverse forces (IF) or ICF depend on the objects extension. Newton's derivation of the theorem is by the use of Euclidean geometry, but the forces between two spherically symmetrical objects can also be derived by the use of algebra.

Let the objects nos. i and j be spherically symmetrical with masses m_i and m_j and with a uniform density within the balls with the radii σ_i and σ_j. The attraction, IF, ISF or ICF, on

a mass δm_i at $\mathbf{s}_i$ in object i and at the distance s_{ij} from a mass δm_j at $\mathbf{s}_j$ in j is

$$\delta\mathbf{F}_{ij} = -\beta\delta m_i\delta m_j s_{ij}^n\hat{\mathbf{s}}_{ij}, \tag{1}$$

with $n=-1$, -2 and -3, respectively, and the total force $\mathbf{F}_{ij}$ is obtained by a quadruple integration, first between δm_i at $\mathbf{s}_i$ and mass elements δm_j in a sphere in j with radius $\sigma_j' \leq \sigma_j$, then over spheres centred at $\mathbf{r}_j$ with radius σ_j' and then correspondingly between mass m_j located in the centre $\mathbf{r}_j$ and mass elements δm_i.

Consider mass elements $\delta m_j(\mathbf{s}_j) = 4\pi\sigma_j'^2 m_j d\sigma_j'/(4\pi/3\sigma_j^3)$ at $\mathbf{s}_j$ in a thin shell $[\sigma_j', \sigma_j' + d\sigma_j']$ with the centre at $\mathbf{r}_j$ and a distance $r_{ij}' =\mid \mathbf{s}_i - \mathbf{r}_j \mid > \sigma_i + \sigma_j \geq \sigma_i + \sigma_j'$ to $\mathbf{s}_i$. The force $\delta\mathbf{F}_{ij} = -\beta\delta m_i m_j s_{ij}^n\hat{\mathbf{r}}_{ij}'$ on δm_i from object j is (Wikipedia Newton shell (2022)

$$\delta\mathbf{F}_{ij} = -\beta\frac{\delta m_i}{4r_{ij}'^2}\int_0^{\sigma_j}\frac{\delta m_j}{\sigma_j'}\int_{r_{ij}'-\sigma_j'}^{r_{ij}'+\sigma_j'} s_{ij}^n[s_{ij}^2 + r_{ij}'^2 - \sigma_j'^2]ds_{ij}\hat{\mathbf{r}}_{ij}'. \tag{2}$$

The integrals are very simple for ISF since

$$-\beta\frac{\delta m_i}{4r_{ij}'^2}\int_0^{\sigma_j}\frac{\delta m_j}{\sigma_j'}\int_{r_{ij}'-\sigma_j'}^{r_{ij}'+\sigma_j'} s_{ij}^{-2}[s_{ij}^2 + r_{ij}'^2 - \sigma_j'^2]ds_{ij}$$
$$= -\beta\frac{\delta m_i}{4r_{ij}'^2}\int_0^{\sigma_j}\frac{\delta m_j}{\sigma_j'}4\sigma_j' = -\beta\frac{\delta m_i m_j}{r_{ij}'^2}, \tag{3}$$

and the integration over shells centred at $\mathbf{r}_i$ with mass elements δm_i leads to *Theorem XXXI*.

The integrations are more complex for $n \neq -2$. The simplest way to proceed is to expand the first integral in powers of σ_j'/r_{ij}'. The first terms in the final expressions for the force between i and j are given in the following.

For the IF function s^{-1}:

$$\mathbf{F}_{ij}(r_{ij}) \simeq -\frac{\beta_1 m_i m_j}{r_{ij}}(1 - \frac{\sigma_i^2 + \sigma_j^2}{5r_{ij}^2})\hat{\mathbf{r}}_{ij} + \mathcal{O}(r_{ij}^{-4}). \tag{4}$$

For s^{-2}, one obtains the usual expression for the gravitational ISF force ($\beta_2 = G$), which does not depend on the extensions of the two spherically symmetrical objects

$$\mathbf{F}_{ij}(r_{ij}) = -\frac{Gm_i m_j}{r_{ij}^2}\hat{\mathbf{r}}_{ij}. \tag{5}$$

For s^{-3}, the ICF radial force is

$$\mathbf{F}_{ij}(r_{ij}) = -\frac{\beta_3 m_i m_j}{r_{ij}^3}(1 + \frac{2\sigma_i^2 + 2\sigma_j^2}{5r_{ij}^2})\hat{\mathbf{r}}_{ij} + \mathcal{O}(r_{ij}^{-6}). \tag{6}$$

The dynamics of planetary systems with the different kinds of gravitational attractions is given in the next section.

3 Dynamics of planetary systems with different gravitational forces

A discrete and exact algorithm for obtaining planetary systems is derived in a recent article (Toxvaerd 2022). The algorithm is symplectic and time reversible and has the same invariances as Newton's analytic dynamics. For Kepler's solution of the two-body system of a Sun
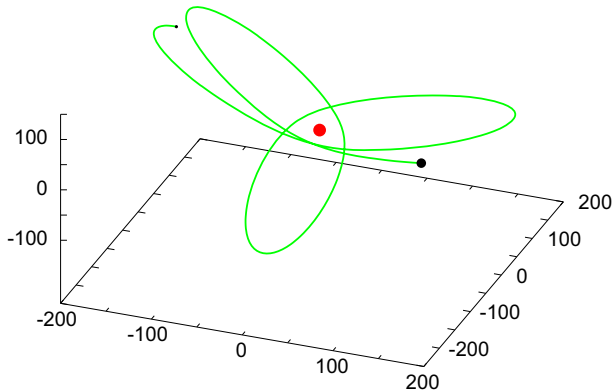
Fig. 1 A loop of the innermost planet from a position at time $t = 2.5 \times 10^6$, marked by a big black sphere to a position at $t = 2.5007325 \times 10^6$ (293000 discrete time steps), marked by a small black sphere. The position of the "Sun" is with an enlarged red sphere. Some simultaneous loops of two other planets in the planetary system are shown in the next figure
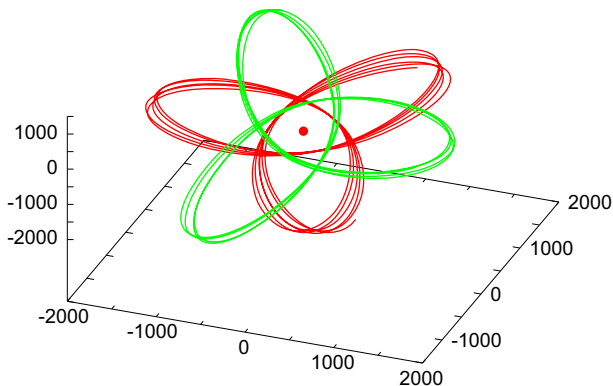

Fig. 2 The simultaneous orbits with bows for two other planets in the planetary system. The orbits are obtained for one million discrete time steps in the time interval $t \in [2.5 \times 10^6, 2.5025 \times 10^6]$

and a planet, one can compare the two dynamics (Toxvaerd 2020), which leads to the same orbits. The discrete dynamics is absolutely stable and without any adjustments for conservation of energy, momentum and angular momentum for billion of time steps. The algorithm and how to obtain the planetary systems are given in Appendix. Here, the algorithm is used to obtain the planetary systems with forces different from the Newtonian inverse-square gravitational forces.

3.1 Planetary systems for objects with inverse forces

The IF between two objects i and j is given by Eq. (4). Equation (4) gives the first-order size correction for the forces between spherically symmetrical uniform mass objects. The investigation is conducted in two ways by MD simulations. *A*: One can simply create the planetary systems in the same way as described in Toxvaerd (2022) and in Appendix, or
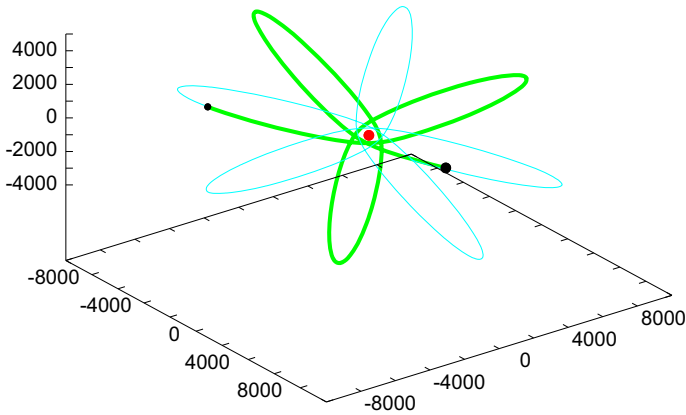
Fig. 3 Bows in a loop with green and light blue for the outermost planet. The start position at $t = 2.5 \times 10^6$ is marked with a big black sphere, and the first three bows are marked with green. The position at $t = 2.5025 \times 10^6$ after the first three bows is shown by a smaller black sphere, and the succeeding five bows are marked with light blue. Several consecutive loops of the planet are shown in Figure 5
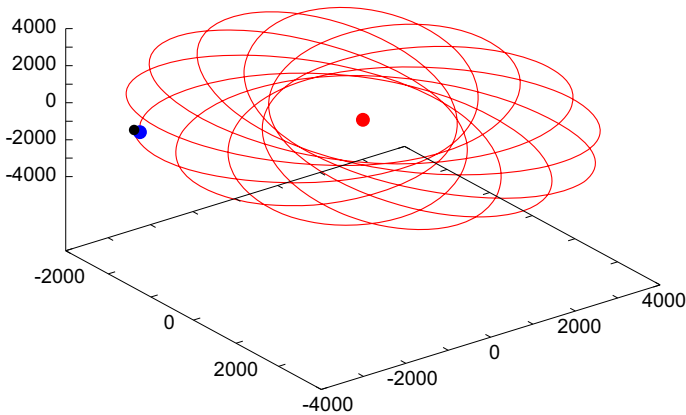

Fig. 4 A planet which after 13 orbits almost returns to its start position. The start position at $t = 2.5 \times 10^6$ is shown with a big blue sphere, and the position at $t = 2.5051975 \times 10^6$ after 13 orbits by a smaller black sphere. The next figure shows several orbits of the planet together with the orbits of the outermost planet

alternatively *B*: one can replace the Newtonian ISF forces between objects in an ordinary planetary system by the corresponding inverse IF forces.

A: The results of obtaining planetary systems spontaneously by merging of objects as in Toxvaerd (2022) are shown in the next figures. The planetary systems with a strength $\beta_1 = 1$ were created spontaneously at time $t = 0$ from different configurations, distributions of velocities and masses $m_i(0) = 1$ of objects. (For units of length, time and strength of the attractions in the MD systems, see Appendix.) Ten different planetary systems were formed, and the overall result and conclusion from the 10 systems is that it is easy to obtain the planetary systems with IF forces. But, the regular orbits deviate, however, qualitatively from the elliptical orbits in an ordinary planetary system. A typical regular orbit is shown in Fig. 1.

Figure 1 shows a loop of the innermost planet in one of the 10 planetary systems, which was simulated with IF. The planetary system was started with thousand objects, and the
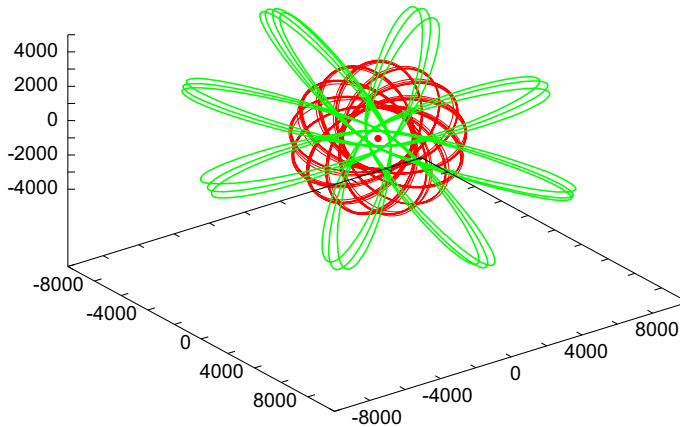
Fig. 5 The outermost planet (green) together with the planet from Fig. 4 (red) with its orbits in bands. The outermost planet changes its major orbit axis with $\approx \pi/4$ at every part of the Sun. The central Sun is marked with red

planetary system with IF contained 38 planets after 10^9 MD time steps corresponding to a MD time $t = 2.5 \times 10^6$, where the inner planets have performed several thousand bound rotations. The planet in Fig. 1 performs a loop, but with a change in its elliptical major axis by $\approx \pi/3$ at the passage of the "Sun", by which the total regular orbit appears with three consecutive bows with an angle of $\approx 2\pi/3$. The total angular momentum for the system is conserved by Newton's exact discrete algorithm (Toxvaerd 2022), but also the angular momentum of the individual planets in the system is conserved to a high degree, so the three bows are in the same plane. Most of the planets exhibit this regular dynamics. Figure 2 shows the simultaneous orbits for two other planets in the same planetary system. The planetary system with the object shown in Figs. 1 and 2 consists of 38 objects in bound orbits around a central heavy object (the "Sun" with m_{Sun}=867). Broucke (1980) has obtained the orbit for one planet (Fig. 2 in Broucke (1980)). There are, however, only some similarities between the present orbits for a many-body three-dimensional planetary system and the 2D orbit of a single planet.

All the planets in the planetary systems with inverse forces show what Newton probably would have called revolving orbits, but not all of the planets have orbits of the form shown in Figs. 1 and 2. Figure 3 shows the consecutive bows of the outermost planet in the same planetary system. The planet changes its principal axis by $\approx \pi/4$ by which it performs eight bows in its regular orbit. Figure 5 shows 3–4 loops of this planet (green) together with another planet in the same planetary system.

It has not been possible to obtain simple elliptical regular orbits, but there are examples of planets with a smaller change in their principal axis at the passage of the Sun. Figure 4 shows such an example of a planet, which after 13 loops returns to its start position, and a collection of consecutive loops for this planet, shown in red in Fig. 5, demonstrates that this regular pattern is maintained over many consecutive loops.

B: Planetary systems with IF forces were obtained in another way by replacing the Newtonian ISF forces in an ordinary planetary system with the IF forces. The discrete dynamics with IF was started with the end positions of the planet in the planetary system (Toxvaerd 2022). A replacement with $\beta_1 = \beta_2 = G$ results in a collapse of the planetary systems and with only two planets in revolving orbits similar to the orbits shown in Fig. 2. The other
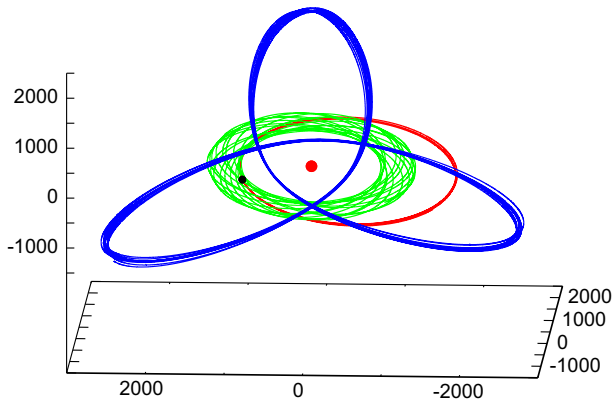
Fig. 6 The red elliptical orbits are for a planet with Newtonian ISF forces and the green orbits are after the forces at the position marked with a black sphere replaced with IF forces and with β_1=0.00105 by which the planet in a short time follows the elliptical path before the revolving behaviour. The orbit (blue) of a planet at a mean distance slightly bigger than the planet shown by red changed spontaneously its elliptical orbit to the bows also shown in the previous figures

planets were engulfed by the Sun. This is due to that the inverse forces with $\beta_1 = \beta_2 = G$ and acting on a planet are about thousand times stronger than the Newtonian gravitational forces. Planets in the Newtonian planetary systems in Toxvaerd (2022) are located at mean distances to their Suns at $< r_{i,Sun} > \approx [100, 30000]$. For an ordinary planetary system with a Newtonian ISF force field and at a position $r_{i,Sun} = 1000$, the corresponding IF force is of the order thousand times stronger than the Newtonian ISF force. So, in order to establish whether it is possible to obtain simple elliptical orbits without revolving orbits, the forces in the Newtonian planetary systems in Toxvaerd (2022) were replaced with IF forces and with $\beta_1 \approx G/1000$. The replacement was performed in the following way:

A planet i with a rather circular orbit and at a mean distance $< r_{i,Sun} > \approx 1000$ was selected, and the strength $\beta_1 = 0.00105$ was determined, so the planet follows the same elliptical orbit shortly after the replacement. The result of this replacement of the forces in the planetary system on the orbit of this planet is shown in Fig. 6, which shows the orbit of an ordinary planetary system before (red) and after (green) the replacement. The replacement is for $\beta = 0.00105$ for which the planet followed the gravitational orbit (red) over a long period of time before it deviated and exhibited the revolving orbits shown in the figure, but with a small change in its principal axis by passage at the Sun and with elliptical-like orbits. The other planet in the Newtonian planetary system changed their orbits to the revolving orbits (blue orbit, Fig. 6), also shown in the previous figures.

It has not been possible to obtain simple elliptical orbits, which spontaneously appears in an ordinary Newtonian planetary system. The simulations were performed by the first-order IF expression, Eq. 4, but simulations with and without the first-order correction $\mid \delta\mathbf{F}_{IF} \mid = \beta_1 m_i m_j (\sigma_i^2 + \sigma_j^2)/5r_{ij}^3$ showed that the first-order correction only has a minor quantitative effect and that the exclusion of this term does not change the overall qualitative result.

3.2 Simulation of systems with inverse cubic forces

A system of objects with masses $m_i(0) = 1$ and pure ICF given by Eq. (6) does not self-assemble to a planetary system. The objects either fuse together or expand as free objects.
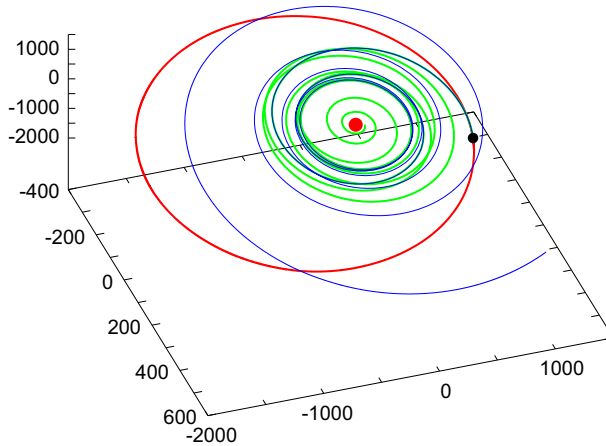
Fig. 7 The orbits for a planet in a planetary system with ICF. The planetary system is obtained from an ordinary planetary system and with elliptical orbits (red) by replacing the ISF forces by ICF and with a strength $\beta_3 \approx 1230 \times G$. The black circles are the position of the planet at the time where the replacement took place, and the green curve is for $\beta_3 = 1228.75$ and the blue curve is for $\beta_3 = 1228.5$

Fig. 8 Top view of the orbits of the planet also shown in detail in the previous figure. The blue curve is ICF with Eq. (6), and the magenta curve is the zero-order ICF $-1228.5 m_i m_j / r_{ij}^3$
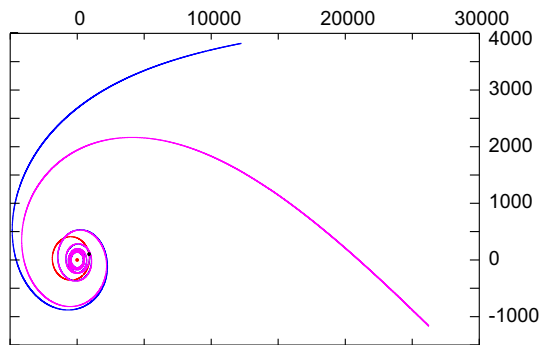
This observation is valid for different values of the gravitational constant β_3 in Eq. (6), and it was not possible to create a planetary system with ICF.

Another way to demonstrate the instability of planetary systems with pure ICF attractions is to replace the Newtonian gravitational ISF in a planetary system by ICF as described in the previous subsection. Thus, it is possible to determine a value of $\beta_3 \pm \delta$, by which a given planet in an Newtonian planetary system either engulfs by the Sun by changing the forces from $-G/r^2$ to $-(\beta_3 + \delta)/r^3(1 + (2\sigma_i^2 + 2\sigma_j^2)/5r_{ij}^2)$ or leaves the Sun as a free object for $\beta_3 - \delta$. Figure 7 shows this "tipping point" for the same planetary system and planet as shown in Fig. 6 in red for ISF and green for IF. The planet with pure ICF is engulfed by the Sun for $\beta_3 + \delta = 1228.75$ (green curve), but escapes the Sun for $\beta_3 - \delta = 1228.5$ (blue curve). Equation (6) shows the first asymptotic correction in a rapid converging expansion for the extension of the spherically symmetrical objects with a uniform density. The zero-order expression for the ICF system: $-\beta_3 m_i m_j / r_{ij}^3$ gives the same qualitatively result, as shown in Fig. 8. The tipping point is the same either one includes the first-order correction or not.
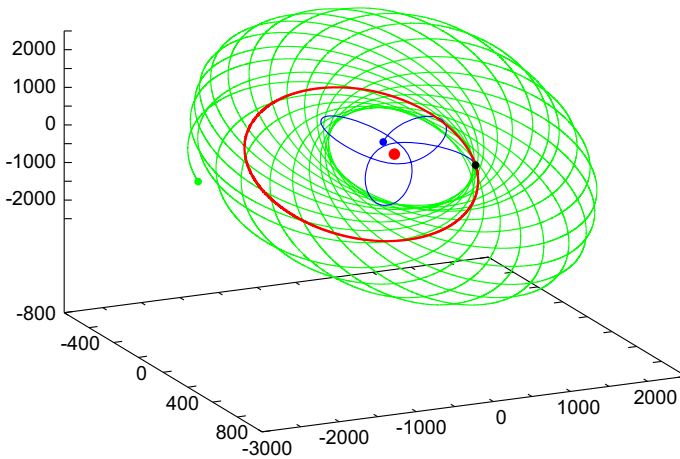
Fig. 9 The planet also shown in Fig. 7 in red, but now with IF or ICF included in the ISF attraction. The orbit in red is with pure ISF; the orbit in green is with ICF: $\alpha_3/r^3 = -100/r^3$ included from the position marked by a black sphere, and the orbit in blue is with the IF: $\alpha_1/r = 0.01/r$ included. The planet with ISF + ICF in green has revolved ≈ 23–24 times before the principal axis in the elliptical orbit has changed 2π

4 Newton's proportions for the Moon's revolving orbits

The Moon exhibits apsidal precession, which is called Saroscyclus, and it has been known since ancient times. Newton showed in Propositions 43–45 in *Principia* that the added force on a single object from a fixed mass centre which can cause its apsidal precession must be a central force between the planet and a mass point fixed in space (the Sun). In Proposition 44, he showed that an inverse cubic force (ICF) might cause the revolving orbits, and in Proposition 45, Newton extended his theorem to arbitrary central forces by assuming that the particle moved in nearly circular orbit (Chandrasekhar 2003). The Moon's apsidal precession is explained by flattering by the rotating Earth with tide waves, which causes an ICF on the Moon. For Newton's analysis of the Moon's apsidal precession, see (Aoki 1992).

New investigations of isotopes from the Moon reveal that it was created ≈ 4.51 billion years ago and ≈ 50 to 60 million years after the emergence of the Earth and our solar system (Barboni et al. 2107; Thiemens et al. 2019), and the Earth contained the Hadean ocean(s) with tide waves shortly after the creation of the Moon (Harrison 2009), so an ICF has not affected the overall stability of the Moon's regular orbit. The rotation of the Earth and the Moon's orbit around the Earth results in an ICF, which has accelerated the Moon out to its present position with its apsidal precession. The early orbit of the Moon may have had a high eccentricity (Garrick-Bethell et al. 2006), but it is difficult to determine the evolution of the Moon's orbit due to the many factors that influence its evolution (Green et al. 2017). One can, however, conclude that the presence of an additional force on the Moon due to the tide waves has not affected the overall stability of the Moon's regular orbit.

The planetary system and the orbit shown in red in Fig. 7 are simulated with either ICF or IF included in the attractions. The planetary system is affected by including an $\alpha_3 r^{-3}$ ICF, and the systems are destroyed for $\alpha_3 \geq 100$. The ISF planetary system with the planet shown in Fig. 7 in red contains 21 planets and only three survived by including $100 * r^{-3}$ in the attraction, whereas all 21 planets remained in regular orbits for ICF with $\alpha_3 \leq 10 * r^{-3}$.

The orbits in a planetary system with ISF+ICF forces exhibit the revolving behaviour predicted by Newton: Fig. 9 shows the orbit of the planet, also shown in Fig. 7, in red without additional attractions, in green with ISF+ICF and with $\alpha_3 = -100$ and in blue with ISF+IF and with $\alpha_1 = 0.01$. The behaviour of ISF+ICF and ISF+IF is in agreement with Newton's *Proposition* 45. Inclusion of IF in the gravitational attractions enhances, however, the revolving behaviour and stabilizes the planetary system, whereas inclusion of the ICF also results in revolving orbits, but it destabilizes the planetary system. The planetary ISF+ICF system is not stable for $\alpha_3 > 100$ and for pure ICF attractions.

5 Conclusion

The discrete algorithm (Appendix A), derived in Toxvaerd (2022), is used to obtain the planetary systems with forces other than gravitational forces. The main conclusion is that it is easy to obtain the planetary systems with inverse gravitational forces. However, it is not possible to obtain the planetary systems with inverse cubic gravitational forces, even if one smoothly replaces the inverse square gravitational forces in a stable planetary system with inverse cubic forces. A detailed investigation of the planetary system after the replacement of the forces shows that one can determine a strength of the gravitational constant β_3 for inverse cubic forces for which a planet either detaches itself from the planetary system for $\beta_3 - \delta$ or is engulfed by the "Sun" for $\beta_3 + \delta$ (Figs. 7 and 8). So, the attractions in our universe with inverse-square forces for the gravitational attractions between masses and the Coulomb attractions between charges are the limit value for regular orbits. A system of objects will, for inverse attractions with $\propto r^{-n}$ with $n \geq 3$, have the well-known thermodynamic behaviour with gas–liquid–solid phases, but without regular orbits between units in the system.

The orbits of the planets in a planetary system with pure inverse forces have "revolving orbits". The regular orbits deviate, however, significantly from the slightly perturbed elliptic orbits in an ordinary planetary system with additional weak non-gravitational attractions. The principal axis changes with $\approx \pi/3$ at every loop (Figs. 1, 2, 6) for the main part of the regular orbits in a planetary system with inverse forces. But, also changes with $\pi/4$ are observed (Figs. 3 and 5) together with other smaller, but rather constant changes (Figs. 4 and 5).

Newton stated in Propositions 43–45 in *Principia* that the Moons revolving orbits could be explained by an additional attraction, r^{-n}, to the gravitational attraction with $n \neq 2$. The present simulations of planetary systems with gravitational attractions and an additional attraction with either $n = 1$ or $n = 3$ confirm Newton's Propositions, but whereas attractions with additional inverse attractions stabilize the planetary systems, the inclusion of a weak inverse cubic attraction also gives "revolving orbits" (Fig. 9), but it will destabilize the planetary system by adding sufficient strong inverse cubic attractions to the inverse-square gravitational forces.

Data Availability Data will be available on request.

Appendix A: Classical discrete dynamics of planetary systems

The gravitational force, $\mathbf{F}_i(\mathbf{r}_i)$, on a planet i at $\mathbf{r}_i$ in a planetary system with N celestial objects is

$$\mathbf{F}_i(\mathbf{r}_i) = \sum_{j \neq i}^{N} \mathbf{F}_{ij}(r_{ij}), \tag{A1}$$

where the summations over forces $\mathbf{F}(r_{ij})$ are given by one of Eqs. 4–6.

Newton derived the discrete central difference algorithm when he obtained his second law (Toxvaerd 2020). In Newton's classical discrete dynamics (Newton 1726; Toxvaerd 2020), a new position $\mathbf{r}_k(t + \delta t)$ at time $t + \delta t$ of an object k with the mass m_k is determined by the force $\mathbf{f}_k(t)$ acting on the object at the discrete positions $\mathbf{r}_k(t)$ at time t and the position $\mathbf{r}_k(t - \delta t)$ at $t - \delta t$ as

$$m_k \frac{\mathbf{r}_k(t + \delta t) - \mathbf{r}_k(t)}{\delta t} = m_k \frac{\mathbf{r}_k(t) - \mathbf{r}_k(t - \delta t)}{\delta t} + \delta t \mathbf{f}_k(t), \tag{A2}$$

where the momenta $\mathbf{p}_k(t + \delta t/2) = m_k(\mathbf{r}_k(t + \delta t) - \mathbf{r}_k(t))/\delta t$ and $\mathbf{p}_k(t - \delta t/2) = m_k(\mathbf{r}_k(t) - \mathbf{r}_k(t - \delta t))/\delta t$ are constant in the time intervals in between the discrete positions. Newton postulated Eq. (A2) and obtained his second law, and the analytic dynamics in the limit $lim_{\delta t \to 0}$.

The algorithm, Eq. (A2), is usually presented as the "leap-frog" algorithm for the velocities

$$\mathbf{v}_k(t + \delta t/2) = \mathbf{v}_k(t - \delta t/2) + \delta t/m_k \mathbf{f}_k(t). \tag{A3}$$

The positions are determined from the discrete values of the momenta/velocities as

$$\mathbf{r}_k(t + \delta t) = \mathbf{r}_k(t) + \delta t \mathbf{v}_k(t + \delta t/2). \tag{A4}$$

Let all the spherically symmetrical objects have the same (reduced) number density $\rho = (\pi/6)^{-1}$ by which the diameter σ_i of the spherical object i is

$$\sigma_i = m_i^{1/3} \tag{A5}$$

and the collision diameter is

$$\sigma_{ij} = \frac{\sigma_i + \sigma_j}{2}. \tag{A6}$$

If the distance $r_{ij}(t)$ at time t between two objects is less than σ_{ij}, the two objects merge to one spherical symmetrical object with a mass

$$m_\alpha = m_i + m_j, \tag{A7}$$

and a diameter

$$\sigma_\alpha = (m_\alpha)^{1/3}, \tag{A8}$$

and with the new object α at the position

$$\mathbf{r}_\alpha(t) = \frac{m_i}{m_\alpha}\mathbf{r}_i(t) + \frac{m_j}{m_\alpha}\mathbf{r}_j(t), \tag{A9}$$

at the centre of mass of the two objects before the fusion. (The object α at the centre of mass of the two merged objects i and j might occasionally be near another object k by which more objects merge, but after the same laws.)

The momenta of the objects in the discrete dynamics just before the fusion are $\mathbf{p}^N(t-\delta t/2)$, and the total momentum of the system is conserved at the fusion if

$$\mathbf{v}_\alpha(t - \delta t/2) = \frac{m_i}{m_\alpha}\mathbf{v}_i(t - \delta t/2) + \frac{m_j}{m_\alpha}\mathbf{v}_j(t - \delta t/2), \tag{A10}$$

which determines the velocity $\mathbf{v}_\alpha(t - \delta t/2)$ of the merged object.

The algorithm for a planetary system consists of equations (A3)+(A4) for time steps without merging objects, and the fusion of objects is given by Eqs. (A6),(A7), (A8), (A9) and (A10).

Newton's discrete algorithm (A3), which is used in almost all MD simulations, is usually called the Verlet or leap-frog algorithm, and it has the same invariances as his exact analytic dynamics (Toxvaerd 2022, 1994; Toxvaerd et al. 2012). The invariances are maintained by the extension to the planetary systems (A6),(A7), (A8), (A9) and (A10) (Toxvaerd 2022) .

The gravitational strengths in the article are in units of $\beta_i^* = G = 1$ and the mass $m_i(0) = 1$ and diameters of the planets $\sigma_i(0) = 1$ at the start time $t = 0$. For units and set-up of the systems, see also (Toxvaerd 2022). The planetary systems in the articles are obtained for thousand objects, which at $t = 0$ are separated with a mean distance $< r_{ij} > \approx 1000$ and with Maxwell–Boltzmann distributed velocities with a mean velocity $< v_i > \approx 1$; for the set-up of the systems, see also (Toxvaerd 2022). The systems are followed at least 10^9 MD time steps, i.e. $t = 2.5 \times 10^6$ time units, which corresponds to $\approx 10^3$ to 10^4 orbits for a planet.

References

Aoki, S.: The Moon-test in Newton's Principia: accuracy of inverse-square law of universal gravitation. Arch. Hist. Exact Sci. **44**, 147 (1992)

Barboni, M., Boehnke, P., Keller, B., Kohl, I., Schoene, B., Young, E. D., McKeegan, K. D.: Early formation of the Moon 4.51 billion years ago. Sci. Adv. **3**: e1602365 (2017)

Bertrand, J.: The théoremè relatif au mouvement d'un point attiré vers un centre fixe. C. R. Acad. Sci. **77**, 849–853 (1873)

Broucke, R.: Notes on the central force r^n. Astrophys. Space Sci. **72**, 33–53 (1980)

Chandrasekhar, S.: Newton's Principia for the common reader. Clarendon Press, Reprint edition (2003)

Garrick-Bethell, I., Wisdom, J., Zuber, M.T.: Evidence for a past high-eccentricity lunar orbit. Science **313**, 652 (2006)

Green, J.A.M., Huber, M., Waltham, D., Buzan, J., Wells, M.: Explicitly modelled deep-time tidal dissipation and its implication for Lunar history. Earth Planet Sci. Lett. **461**, 46 (2017)

Harrison, T.M.: The Hadean crust: evidence from >4 Ga Zircons. Annu. Rev. Earth Planet Sci. **37**, 479 (2009)

Mahomed, F.M., Vawda, F.: Application of symmetries to central force problems. Nonlinear Dyn. **21**, 307–315 (2000)

Newton, I.: Philosophiæ naturalis principia mathematica. Londini, Anno MDCLXXXVII. Second Ed.1713; Third Ed. 1726

Principia, Proportion 43-45

Principia, Theorem XXXI

Thiemens, M.M., Sprung, P., Fonseca, R.O.C., Leitzke, F.P., Münker, C.: Early Moon formation inferred from hafnium-tungsten systematics. Nat. Geosci. **12**, 696 (2019)

Toxvaerd, S.: Hamiltonians for discrete dynamics. Phys. Rev. E **50**, 2271 (1994)

Toxvaerd, S.: Newton's disctret dynamics. Eur. J. Phys. **135**, 267 (2020)

Toxvaerd, S.: An algorithm for coalescence of classical objects and formation of planetary systems. Eur. Phys. J. Plus **137**, 99 (2022)

Toxvaerd, S., Heilmann, O.J., Dyre, J.C.: Energy conservation in molecular dynamics simulations of classical systems. J. Chem. Phys. **136**, 224106 (2012)

Whittaker, E. T.: A Treatise on the Analytical Dynamics of Particles and Rigid Bodies, with an Introduction to the Problem of Three Bodies (4th ed.). New York: Dover Publications

Wikipedia Newton shell.: Wikipedia: Newton's shell theorem (2022)